AMERICAN SOCIETY FOR MICROBIOLOGY | Journal of Bacteriology®

RESEARCH ARTICLE

Genetic, Biochemical, and Molecular Characterization of *Methanosarcina barkeri* Mutants Lacking Three Distinct Classes of Hydrogenase

Thomas D. Mand,[a] Gargi Kulkarni,[a]* William W. Metcalf[a]

[a]Department of Microbiology, University of Illinois at Urbana-Champaign, Urbana, Illinois, USA

ABSTRACT The methanogenic archaeon *Methanosarcina barkeri* encodes three distinct types of hydrogenase, whose functions vary depending on the growth substrate. These include the F_{420}-dependent (Frh), methanophenazine-dependent (Vht), and ferredoxin-dependent (Ech) hydrogenases. To investigate their physiological roles, we characterized a series of mutants lacking each hydrogenase in various combinations. Mutants lacking Frh, Vht, or Ech in any combination failed to grow on H_2-CO_2, whereas only Vht and Ech were essential for growth on acetate. In contrast, a mutant lacking all three grew on methanol with a final growth yield similar to that of the wild type and produced methane and CO_2 in the expected 3:1 ratio but had a ca. 33% lower growth rate. Thus, hydrogenases play a significant, but nonessential, role during growth on this substrate. As previously observed, mutants lacking Ech failed to grow on methanol-H_2 unless they were supplemented with biosynthetic precursors. Interestingly, this phenotype was abolished in the Δ*ech* Δ*frh* and Δ*ech* Δ*frh* Δ*vht* mutants, consistent with the idea that hydrogenases inhibit methanol oxidation in the presence of H_2, which prevents production of the reducing equivalents needed for biosynthesis. Quantification of the methane and CO_2 produced from methanol by resting cell suspensions of various mutants supported this conclusion. On the basis of the global transcriptional profiles, none of the hydrogenases were upregulated to compensate for the loss of the others. However, the transcript levels of the F_{420} dehydrogenase operon were significantly higher in all strains lacking *frh*, suggesting a mechanism to sense the redox state of F_{420}. The roles of the hydrogenases in energy conservation during growth with each methanogenic pathway are discussed.

IMPORTANCE Methanogenic archaea are key players in the global carbon cycle due to their ability to facilitate the remineralization of organic substrates in many anaerobic environments. The consequences of biological methanogenesis are far-reaching, with impacts on atmospheric methane and CO_2 concentrations, agriculture, energy production, waste treatment, and human health. The data presented here clarify the *in vivo* function of hydrogenases during methanogenesis, which in turn deepens our understanding of this unique form of metabolism. This knowledge is critical for a variety of important issues ranging from atmospheric composition to human health.

KEYWORDS *Methanosarcina*, hydrogenases, methane, methanogenesis

The ability to metabolize molecular hydrogen (H_2) is a key metabolic feature in methanogenic *Archaea* (1). This trait is conferred by a class of enzymes known as hydrogenases, which catalyze the reversible oxidation of H_2 coupled to various electron donors/acceptors (2, 3). At least five distinct types of hydrogenases are found in methanogenic *Archaea*. These enzymes differ with respect to their redox partners, their cellular localization, and whether their activity is linked to the production or consump-

Received 5 June 2018 **Accepted** 11 July 2018

Accepted manuscript posted online 16 July 2018

Citation Mand TD, Kulkarni G, Metcalf WW. 2018. Genetic, biochemical, and molecular characterization of *Methanosarcina barkeri* mutants lacking three distinct classes of hydrogenase. J Bacteriol 200:e00342-18. https://doi.org/10.1128/JB.00342-18.

Editor Anke Becker, Philipps-Universität Marburg

Address correspondence to William W. Metcalf, metcalf@life.illinois.edu.

* Present address: Gargi Kulkarni, California Institute of Technology, Pasadena, California, USA.

T.D.M. and G.K. contributed equally to this article.

For a commentary on this article, see https://doi.org/10.1128/JB.00445-18.

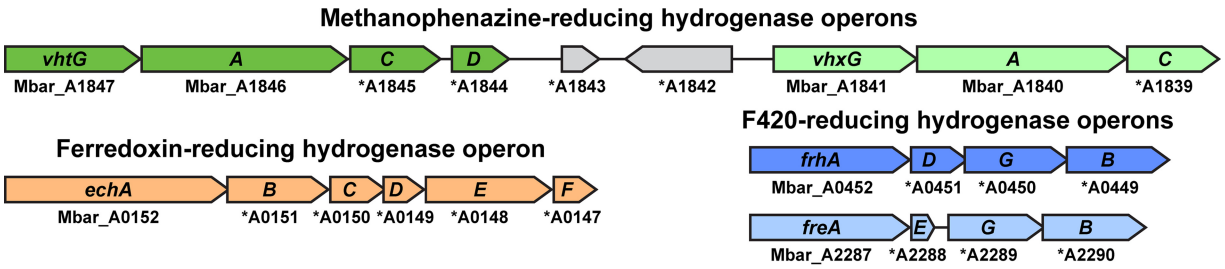

FIG 1 Hydrogenase operons of *Methanosarcina barkeri*. Three distinct types of hydrogenase are encoded by *M. barkeri*. Two potential methanophenazine-dependent hydrogenases are encoded by the adjacent *vhtGACD* and *vhxGAC* operons, while two potential F_{420}-dependent hydrogenases are encoded by the unlinked *frhADGB* and *freAEGB* operons. The energy-converting, ferredoxin-dependent hydrogenase is encoded by the *echABCDEF* operon. Locus tags are shown below each gene, in some cases the "Mbar_" prefix was omitted (shown by an asterisk) due to space constraints.

tion of the membrane potential (4). Biochemical characterization of these diverse hydrogenases led to proposed functions for each enzyme class that differ substantially between methanogens with and without cytochromes (5).

Methanogens without cytochromes produce at least four types of hydrogenase, including (i) the electron-bifurcating Mvh hydrogenase, which couples oxidation of hydrogen to reduction of ferredoxin (Fd) and a mixed coenzyme M (CoM)-coenzyme B (CoB) disulfide, (ii) the coenzyme F_{420}-dependent hydrogenase, (iii) the [Fe] hydrogenase, which couples hydrogen oxidation to reduction of methenyltetrahydromethanopterin, and (iv) the ferredoxin-dependent, energy-converting hydrogenases (4). The first three are cytoplasmic enzymes, which supply the electrons needed to reduce CO_2 to methane. The last is a membrane-bound multisubunit complex that couples hydrogenase activity to the production/consumption of the ion motive force across the cell membrane (hence the designation "energy converting"). In non-cytochrome-containing methanogens, these energy-converting hydrogenases are believed to provide low-potential electrons, in the form of reduced ferredoxin, needed for anaplerotic reactions (6).

Methanogens with cytochromes, typified by *Methanosarcina barkeri*, encode a different set of hydrogenases that includes one cytoplasmic enzyme and two membrane-bound enzymes (Fig. 1) (7). Like the non-cytochrome-containing methanogens, *M. barkeri* produces a cytoplasmic, three-subunit F_{420}-dependent hydrogenase known as Frh (for F_{420}-reducing hydrogenase). Frh is encoded by the four-gene *frhADGB* operon, which encodes the α, β, and γ subunits (FrhA, FrhB, and FrhG, respectively), along with the maturation protease FrhD (8). A second locus, *freAEGB*, encodes proteins that are 86 to 88% identical to FrhA, FrhB, and FrhG but lacks the gene for the maturation protease FrhD, instead encoding a small protein of unknown function (FrhE). It is not known whether the *fre* operon is capable of producing an active hydrogenase (8–11). A membrane-bound hydrogenase linked to the quinone-like electron carrier methanophenazine has, to date, been found only in *Methanosarcina* species. This enzyme, known as Vht, because it was initially identified as a viologen-reducing hydrogenase (two), is encoded by the *vhtGACD* operon, which encodes the biochemically characterized enzyme comprised of VhtA and VhtG, along with a putative membrane-bound cytochrome, VhtC, that does not copurify with the active enzyme, and a maturation protease, VhtD (7). As with the F_{420}-reducing hydrogenase, a second locus that lacks the maturation protease is encoded in *M. barkeri* strains. This operon (*vhxGAC*) encodes proteins that display ca. 50% amino acid sequence identity with those encoded by *vhtGACD*. Like *freAEGB*, it is not known whether the *vhx* operon produces an active hydrogenase (7). Finally, *M. barkeri* encodes a membrane-bound, ferredoxin-dependent energy-converting hydrogenase (Ech) (12). This five-subunit enzyme complex is much simpler than and only distantly related to the energy-converting hydrogenases of the non-cytochrome-containing methanogens, which typically contain more than a dozen subunits (3). Homologs of the electron-bifurcating and

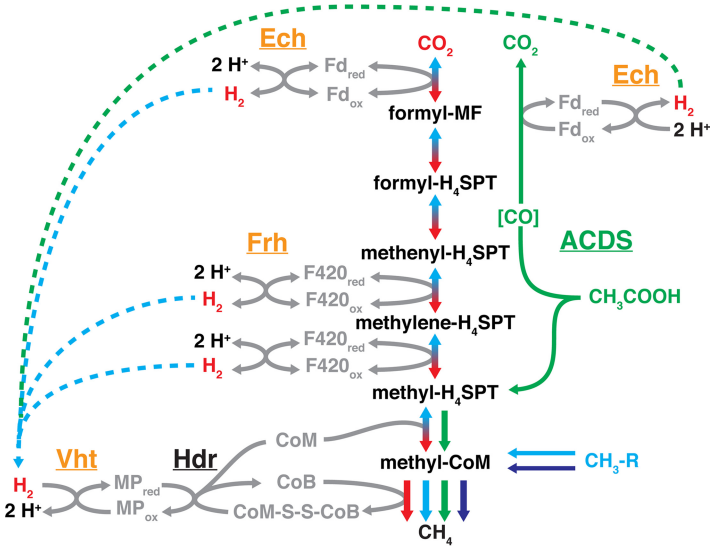

FIG 2 Four methanogenic pathways of *Methanosarcina*. Each pathway shares a common step in the reduction of methyl-CoM to methane; however, they differ in the route used to form methyl-CoM and in the source of electrons used for its reduction to methane. The CO_2 reduction pathway (red arrows) involves the reduction of CO_2 to methane using electrons derived from the oxidation of H_2, while the methylotrophic pathway (light blue arrows) involves disproportionation of C_1 substrates to methane and CO_2. These two pathways share many steps, with overall metabolic flux occurring in opposite directions (shown by red- and light blue-shaded arrows). In the aceticlastic pathway (green arrows), acetate is split into a methyl group and an enzyme-bound carbonyl moiety (shown in brackets) by the enzyme acetyl-CoA decarbonylase/synthase (ACDS). The latter is oxidized to CO_2, producing reduced ferredoxin that provides electrons for reduction of the methyl group to methane. Lastly, in the methyl reduction pathway (dark blue arrows), C_1 compounds are reduced to CH_4 using electrons derived from H_2 oxidation. Dashed lines depict the diffusion of H_2, which occurs during the transfer of electrons between the oxidative and reductive portions of the methylotrophic and aceticlastic pathways. The steps catalyzed by the Frh, Vht, and Ech hydrogenases are indicated. Note that in wild-type *M. barkeri*, hydrogenases are involved in all four pathways. Abbreviations: Hdr, heterodisulfide reductase; MF, methanofuran; H_4SPT, tetrahydrosarcinapterin; CoM, coenzyme M; CoB, coenzyme B; CoM-S-S-CoB, heterodisulfide of CoM and CoB; Fd_{ox} and Fd_{red}, oxidized and reduced ferredoxin, respectively; $F420_{ox}$ and $F420_{red}$, oxidized and reduced cofactor F_{420}, respectively; MP_{ox} and MP_{red}, oxidized and reduced methanophenazine, respectively.

methenyltetrahydromethanopterin-reducing hydrogenases are not known to occur in cytochrome-containing methanogens.

A key difference between the cytochrome-containing and non-cytochrome-containing methanogens is the ability of the former to use one-carbon (C_1) compounds and acetic acid, in addition to H_2 and CO_2, as growth substrates. Catabolism of these chemically diverse substrates involves four distinct methanogenic pathways: the CO_2 reduction pathway, the methyl reduction pathway, the methylotrophic pathway, and the aceticlastic pathway (13, 14). While several of these pathways share common steps, they differ substantially with respect to the involvement of key enzymes and the direction of metabolic flux during methane production (Fig. 2). Surprisingly, it now appears that some *Methanosarcina* species (e.g., *M. barkeri*) use hydrogenases in each of the four pathways, regardless of whether external H_2 is provided as a growth substrate (15).

During the CO_2 reduction pathway, wherein CO_2 is reduced to CH_4 in a stepwise manner, hydrogenases produce the electron-donating cofactors required for four distinct reduction steps (Fig. 2) (5). Initial reduction of CO_2 to formyl-methanofuran requires reduced Fd (Fd_{red}), which is produced by Ech. This reaction is dependent on an ion motive force because the reduction of Fd by H_2 is endergonic under physiological conditions (16). Subsequent reduction of methenyl-tetrahydrosarcinapterin (H_4SPT) to methylene-H_4SPT and of methylene-H_4SPT to methyl-H_4SPT requires reduced coenzyme F_{420} ($F_{420/red}$), which is supplied by Frh. Finally, reduction of a methyl group to methane using coenzyme B produces a heterodisulfide of coenzyme M and

coenzyme B (CoM-S-S-CoB), which must be reduced to produce the free CoM and CoB needed for continued methanogenesis. This reaction is catalyzed by a membrane-bound heterodisulfide reductase (HdrED), which uses the reduced form of a membrane-bound cofactor, methanophenazine, as the source of electrons (17). H_2, in turn, serves as the reductant for the generation of reduced methanophenazine via membrane-bound Vht hydrogenase. Thus, all three types of hydrogenase are predicted to be required for growth via CO_2 reduction, a conclusion that has been validated by the phenotypic analysis of single mutants (11, 15, 16).

In contrast, methanogenesis via the methyl reduction pathway is expected to require only Vht. In this pathway, the methyl-CoM derived from C_1 compounds, such as methanol or methylamines, is directly reduced to methane using CoB as the electron donor. As with the CO_2 reduction pathway, this produces a CoM-S-S-CoB disulfide that must be regenerated in a pathway requiring HdrDE and reduced methanophenazine, which is presumably generated by Vht (Fig. 2). This idea is supported by the analysis of conditional *vht* mutants (15). Neither Frh nor Ech is required for methanogenesis in this model, a finding that is consistent with experimental data from Δ*frh* and Δ*ech* mutants (11, 16). Nevertheless, the *M. barkeri* Δ*ech* strain cannot grow via the methyl reduction pathway unless the media are supplemented with the biosynthetic precursors. The required precursors can be provided by a mixture of 0.1% yeast extract (YE), 0.1% Casamino Acids (CAA), 10 mM acetate, and 10 mM pyruvate; however, high concentrations of pyruvate alone (100 mM) also serve to bypass the biosynthetic block (16). Thus, Ech plays an essential biosynthetic role under these conditions, which is probably the H_2-dependent synthesis of reduced ferredoxin needed for the synthesis of acetyl coenzyme A (acetyl-CoA) and pyruvate (16).

During aceticlastic methanogenesis, both the Ech and Vht hydrogenases play a critical role in methanogenesis. In this pathway, acetyl-CoA is split into methyl-H_4SPT and enzyme-bound [CO] by the acetyl-CoA decarbonylase/synthase (ACDS) enzyme complex. CO is then further oxidized to CO_2 with the concomitant reduction of ferredoxin (12, 16). It is believed that the exergonic oxidation of ferredoxin by Ech produces H_2 and contributes to the proton motive force by transferring protons across the membrane. The proton motive force is further enhanced by a putative H_2 cycling mechanism, in which the H_2 produced by Ech diffuses across the membrane, where it is oxidized by Vht to produce reduced methanophenazine. This unusual electron transport chain is completed when the reduced methanophenazine produced by Vht is used by HdrDE to regenerate free CoM and CoB from the CoM-S-S-CoB heterodisulfide (Fig. 2) (18). Participation of these hydrogenases in the aceticlastic pathway is supported by mutagenic studies showing that *ech* and *vht* mutants do not grow with acetate as the sole substrate, regardless of whether biosynthetic precursors were supplied (15, 16).

Finally, all three types of hydrogenases are thought to be involved in methylotrophic methanogenesis via an H_2 cycling mechanism similar to that described for aceticlastic growth (15). In this pathway, $F_{420/red}$ and Fd_{red}, produced by the stepwise oxidation of methyl groups to CO_2, are converted to molecular H_2 by Frh and Ech, respectively (Fig. 2). H_2 then diffuses to the outer surface of the cell membrane, where it is oxidized by Vht, releasing protons on the outside the cell and contributing to the generation of an ion motive force (Fig. 3) (15). Electrons from the oxidation of H_2 are used to regenerate CoM and CoB via HdrDE, as described above for the aceticlastic pathway. Nevertheless, *M. barkeri* Δ*frh* and Δ*ech* strains are capable of methylotrophic growth, indicating the presence of alternative pathways for the transfer of electrons from $F_{420/red}$ and Fd_{red} to the electron transport chain (11, 16). The membrane-bound F_{420} dehydrogenase complex (Fpo) has been identified as the alternate mechanism of electron transfer from $F_{420/red}$ (11). This enzyme couples the exergonic reduction of methanophenazine by $F_{420/red}$ with the generation of a proton motive force in an H_2-independent manner. However, the *M. barkeri* Δ*frh* strain exhibits lower growth rates than wild-type *M. barkeri*, showing that the H_2-independent electron transport chain is less effective than electron transport via H_2 cycling. The observation that Δ*fpo*

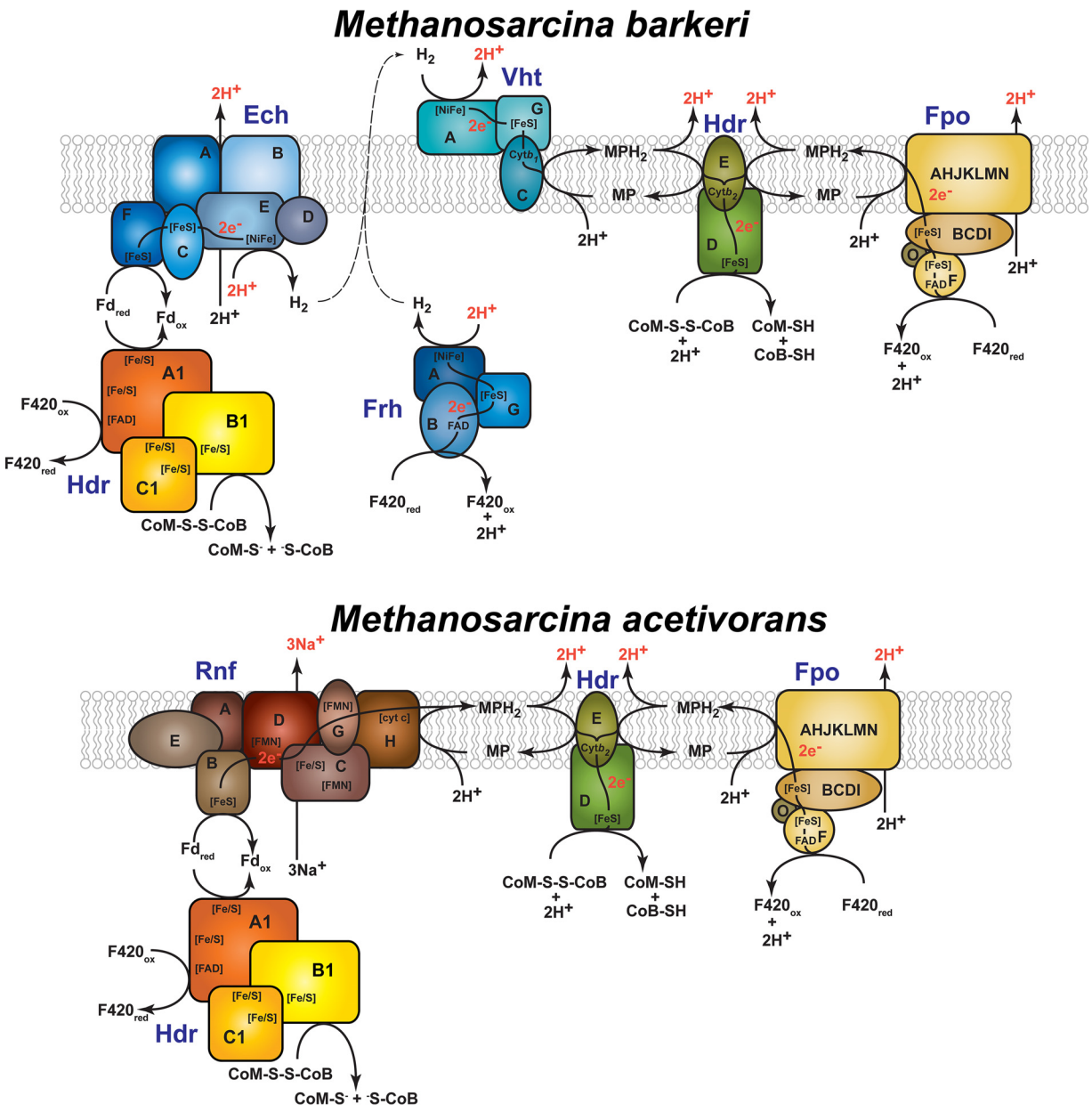

FIG 3 The branched electron transport systems of *Methanosarcina barkeri* and *Methanosarcina acetivorans*. During methylotrophic methanogenesis, *M. barkeri* can utilize H_2-dependent or H_2-independent electron transport systems. The H_2-dependent pathway involves the use of the hydrogenases Frh, Ech, and Vht in an H_2 cycling mechanism to transfer electrons from $F_{420/red}$ or Fd_{red} to methanophenazine (MP). *M. acetivorans* does not utilize hydrogenases and is therefore incapable of H_2 cycling. Both organisms can conserve energy via an H_2-independent pathway, wherein electrons are transferred from $F_{420/red}$ to methanophenazine by way of the F_{420} dehydrogenase (Fpo). Additionally, the electron transport system in *M. acetivorans* includes the Na^+-translocating Rnf enzyme complex that serves as an Fd:methanophenazine oxidoreductase. Both membrane-bound electron transport systems converge at the reduction of the CoM-S-S-CoB heterodisulfide with electrons from reduced methanophenazine via the cytochrome-containing HdrDE enzyme. Protons (or Na^+, in the case of Rnf) are translocated across the cell membrane in both systems, thereby conserving energy in the form of an ion motive force. An additional heterodisulfide reductase, HdrA1B1C1, has been proposed to function in the energy conservation pathways for both organisms. This electron-bifurcating enzyme potentially reduces both the CoM-S-S-CoB heterodisulfide and F_{420} with electrons from Fd_{red} at a stoichiometric ratio of 2 Fd_{red} oxidized for the reduction of 1 CoM-S-S-CoB to CoM-SH/CoB-SH and the reduction of 1 $F_{420/ox}$ to $F_{420/red}$. Abbreviations: Fd_{ox} and Fd_{red}, oxidized and reduced ferredoxin, respectively; MP and MPH_2, oxidized and reduced methanophenazine, respectively; $F420_{ox}$ and $F420_{red}$, oxidized and reduced F_{420}, respectively; CoM, coenzyme M; CoB, coenzyme B; CoM-S-S-CoB, heterodisulfide of CoM and CoB; FeS, iron-sulfur cluster; FAD, flavin adenine dinucleotide; FMN, flavin mononucleotide; NiFe, nickel-iron active site of hydrogenases; Cytb_1, Cytb_2, and cyt c, cytochromes b_1, b_2, and *c*, respectively.

Δ*frh* double mutants are incapable of methylotrophic growth shows that additional electron transport routes are either not present or not sufficient for methylotrophic growth (11). Mutants lacking Vht are inviable under all growth conditions, including methylotrophic growth, unless Frh is also removed. This phenotype is probably due the inability to recapture the H_2 produced in the cytoplasm, which causes a redox imbalance and cell lysis (15).

Although the three *M. barkeri* hydrogenases have been studied *in vitro* and in certain mutants, a complete analysis of their role during growth on various substrates has yet to be reported. In this study, all five hydrogenase operons were systematically deleted in all viable combinations, and the physiological ramifications of these mutations were examined by measuring growth, methanogenesis, and hydrogenase activity on various growth substrates. We also performed global transcriptional profiling to assess the possibility that alternate electron transport chain components are upregulated to compensate for the loss of specific hydrogenases. The data suggest that hydrogenases are not required for methylotrophic methanogenesis but are essential for CO_2-reductive, methyl-reductive, and aceticlastic methanogenesis. Additionally, an inhibitory effect of H_2 on the methyl oxidative pathway appears to be mediated by all three hydrogenases.

RESULTS

Construction of hydrogenase deletion mutants. To assess the role of the *M. barkeri* hydrogenases during growth on various substrates, we constructed mutants lacking the *frhADGB*, *freAEGB*, *vhtGACD*, *vhxGAC*, and *echABCDEF* operons individually and in all possible combinations (see Fig. S1 in the supplemental material). Because mutants lacking *vht* are viable only when *frh* is deleted first (15), we also created a series of conditional mutants that have the *vht* promoter replaced by the synthetic P_{tet} promoter, which is expressed in the presence of tetracycline (Tet) and which is tightly repressed in its absence (19). To simplify the isolation of strains lacking the adjacent *vht* and *vhx* loci, we constructed a mutant allele (denoted Δ*vht-vhx*) in which both operons along with two intervening genes that encode a putative peptidoglycan binding protein (Mbar_A1842) and an uncharacterized hypothetical protein (Mbar_A1843) were deleted. The full set of strains containing deletions of hydrogenase operons in all possible combinations was successfully generated and verified by either Southern hybridization or PCR (Fig. S3 to S6).

Characterization of growth phenotypes in hydrogenase deletion mutants. The generation time, growth yield, and duration of the lag phase for each mutant were determined by monitoring the optical density (OD) during growth in a variety of media, providing clues as to the function of each hydrogenase during the utilization of various carbon and energy sources (Table 1; Fig. S2). With the exception of the Δ*fre* and Δ*vhx* mutations, in which the mutants had no discernible phenotypes alone or in combination with other gene deletions, each of the mutations caused significant growth defects in one or more media.

Strains containing the Δ*ech* mutation were unable to grow in either H_2-CO_2 or acetate medium, regardless of whether the other hydrogenase genes were deleted. However, with the exception of the P_{tet} *vht* Δ*ech* mutant, discussed below, all these mutants grew on methanol medium, albeit with reduced growth rates. Consistent with previous reports, the Δ*ech* single mutant was unable to grow on methanol-H_2-CO_2, unless the medium was supplemented with biosynthetic precursors, such as acetate and pyruvate (16). Interestingly, the Δ*ech* Δ*frh* double mutant regained the ability to grow in this medium, but with a diminished rate and yield and the longest lag phase observed in any of our experiments. These phenotypes were substantially minimized in the Δ*ech* Δ*frh* Δ*vht* triple mutant, suggesting that both Frh and Vht inhibit methanol oxidation, which is needed to provide reducing equivalents for biosynthesis, when H_2 is present.

As previously reported, we were unable to obtain a mutant lacking only *vht*, suggesting that loss of this locus is lethal in otherwise wild-type strains (15). This

TABLE 1 Growth of *M. barkeri* mutant strains on various methanogenic substrates

Genotype	H_2-CO_2			Methanol			Methanol-H_2-CO_2			Acetate		
	Gen. (h)[d]	Max. OD[e]	Lag (h)	Gen. (h)	Max. OD[e]	Lag (h)	Gen. (h)	Max. OD[e]	Lag (h)	Gen. (h)	Max. OD[f]	Lag (h)
Δ*hpt*[a]	10.4 ± 0.7	0.42 ± 0.04	49 ± 11	8.9 ± 0.3	0.85 ± 0.05	36 ± 1	6.2 ± 0.5	0.77 ± 0.03	33 ± 1	43.6 ± 2.2	1.65 ± 0.04	195 ± 11
Δ*fre*	10.3 ± 0.6	0.35 ± 0.03	59 ± 1	8.8 ± 0.4	0.78 ± 0.04	37 ± 1	7.0 ± 0.4	0.68 ± 0.01	38 ± 4	38.6 ± 2.3	1.68 ± 0.05	200 ± 13
Δ*vhx*	10.7 ± 0.5	0.45 ± 0.02	60 ± 3	8.5 ± 0.2	0.78 ± 0.08	36 ± 2	7.5 ± 0.5	0.69 ± 0.04	51 ± 3	47.2 ± 3.8	1.70 ± 0.08	181 ± 22
Δ*ech*	NG[g]	NA[h]	NA	12.2 ± 0.9	0.69 ± 0.05	46 ± 1	NG	NA	NA	NG	NA	NA
Δ*ech* Δ*frh*	NG	NA	NA	12.1 ± 0.7	0.80 ± 0.05	54 ± 2	13 ± 2	0.54 ± 0.03	248 ± 17	NG	NA	NA
Δ*ech* Δ*frh* Δ*vht*	NG	NA	NA	10.8 ± 0.2	0.71 ± 0.06	48 ± 3	9.0 ± 0.4	0.61 ± 0.02	48 ± 2	NG	NA	NA
Δ*ech* Δ*frh* Δ*fre* Δ*vht-vhx*[c]	NG	NA	NA	12.1 ± 0.2	0.84 ± 0.06	54 ± 2	9.3 ± 0.1	0.68 ± 0.03	45 ± 1	NG	NA	NA
P_{tet} *vht*[b]	NG	NA	NA	NG	NA	NA	NG	NA	NA	NG	NA	NA
P_{tet} *vht* Δ*ech*[b]	NG	NA	NA	NG	NA	NA	NG	NA	NA	NG	NA	NA
Δ*frh* Δ*vht*	NG	NA	NA	11.7 ± 0.7	0.89 ± 0.01	54 ± 2	35 ± 3	0.33 ± 0.03	151 ± 4	NG	NA	NA
Δ*frh* Δ*fre* Δ*vht-vhx*[c]	NG	NA	NA	12.3 ± 0.6	0.84 ± 0.07	58 ± 2	29 ± 2	0.43 ± 0.03	116 ± 3	NG	NA	NA
Δ*frh*	NG	NA	NA	19.5 ± 1.0	0.69 ± 0.05	122 ± 6	7.4 ± 0.6	0.64 ± 0.14	45 ± 3	38.2 ± 1.7	1.71 ± 0.03	219 ± 11
Δ*frh* Δ*fre*	NG	NA	NA	16.5 ± 0.8	0.80 ± 0.00	89 ± 2	7.7 ± 0.2	0.74 ± 0.01	48 ± 1	39.6 ± 2.9	1.63 ± 0.07	170 ± 13

[a]The *M. barkeri* Fusaro parental strain.
[b]Growth in the absence of tetracycline.
[c]*Mbar_A1842* and *Mbar_1843* were also deleted.
[d]Gen., generation (doubling) time.
[e]The maximum (max.) optical density at 600 nm was measured on a Spectronic 20 spectrophotometer.
[f]The maximum (max.) optical density at 600 nm was measured on a Hewlett Packard 8453 spectrophotometer. Note that an OD of 1.0 on the Hewlett Packard 8453 spectrophotometer is equivalent to an OD of ~0.2 on the Spectronic 20 spectrophotometer.
[g]NG, no growth for at least 6 months of incubation.
[h]NA, not applicable.

TABLE 2 Production of CH_4 and CO_2 observed from resting cell suspensions of *M. barkeri* mutant strains[e]

	H_2-CO_2		Methanol			Methanol-H_2		
Genotype	CH_4 production (μmol)	CO_2 production (μmol)	CH_4 production (μmol)	CO_2 production (μmol)	CH_4/CO_2[c]	CH_4 production (μmol)	CO_2 production (μmol)	CH_4/CO_2
Δ*hpt*[a]	307 ± 24	NA[d]	339 ± 6	118 ± 2	2.9:1	458 ± 6	<1	
Δ*fre*	316 ± 16	NA	339 ± 7	117 ± 2	2.9:1	442 ± 24	<1	
Δ*vhx*	328 ± 21	NA	329 ± 7	113 ± 3	2.9:1	453 ± 6	<1	
Δ*ech*	5 ± 1	NA	331 ± 6	109 ± 2	3.0:1	460 ± 12	<1	
Δ*ech* Δ*frh*	3 ± 0	NA	328 ± 7	107 ± 2	3.1:1	440 ± 14	4 ± 1	110:1
Δ*ech* Δ*frh* Δ*vht*	1 ± 0	NA	315 ± 5	93 ± 1	3.4:1	313 ± 5	92 ± 2	3.4:1
Δ*ech* Δ*frh* Δ*fre* Δ*vht-vhx*[b]	1 ± 0	NA	314 ± 2	94 ± 1	3.3:1	315 ± 8	93 ± 3	3.4:1
Δ*frh*	34 ± 1	NA	310 ± 8	96 ± 2	3.2:1	442 ± 4	<1	
Δ*frh* Δ*fre*	10 ± 2	NA	298 ± 13	98 ± 4	3.0:1	436 ± 8	<1	
Δ*frh* Δ*vht*	6 ± 1	NA	311 ± 5	92 ± 1	3.4:1	225 ± 16	20 ± 1	11:1
Δ*frh* Δ*fre* Δ*vht-vhx*[b]	5 ± 0	NA	309 ± 6	92 ± 2	3.4:1	300 ± 8	19 ± 1	16:1

[a]The *M. barkeri* Fusaro parental strain.
[b]*Mbar_A1842* and *Mbar_1843* were also deleted.
[c]When relevant, the ratio of CH_4/CO_2 is shown.
[d]NA, not applicable, as the CO_2 produced could not be differentiated from the CO_2 that was added to the headspace.
[e]CH_4 and CO_2 quantities were below 4 ± 1 μmol for each strain when measured in cell suspensions without substrate.

conclusion was supported by the phenotype of the P_{tet} *vht* and P_{tet} *vht* Δ*ech* mutants, which were incapable of growth on any medium when tetracycline was absent (i.e., under repressing conditions). However, as noted above, when cells were grown on methanol, it was possible to delete the *vht* operon if *frh* was deleted first. The Δ*frh* Δ*vht* strains, including ones that also carried an *ech* deletion, had methanol growth phenotypes similar to that of the wild type. Thus, hydrogenases are not required for growth on methanol, although *vht*-deficient strains are inviable in the presence of an active Frh hydrogenase. In contrast, strains lacking *vht* alone or in combination with other mutations were unable to grow on either H_2-CO_2 or acetate medium. A more graded response was observed when various *vht* mutants were grown on methanol-H_2-CO_2. Accordingly, on this substrate combination, the *vht* single mutant was inviable, while the Δ*frh* Δ*vht* double mutant grew very poorly and the Δ*ech* Δ*frh* Δ*vht* strain had phenotypes that were nearly the same as the wild-type phenotype. Again, these data are consistent with the idea that with certain mutant backgrounds Frh, Vht, and Ech inhibit methanol oxidation in the presence of H_2.

Finally, mutants lacking only the *frh* operon grew on three out of four substrates tested, failing to grow only on H_2-CO_2 medium. When methanol was the sole substrate, the Δ*frh* mutant had an extended lag phase and a generation time approximately double that of the parental strain. However, during growth on either acetate or methanol-H_2-CO_2, the growth phenotypes of this strain were equivalent to those of the parental strain, suggesting that Frh enhances growth on methanol but is not required for growth on the two latter substrate combinations.

Methane and CO_2 production by hydrogenase deletion mutants. To probe the underlying mechanisms behind the growth phenotypes, we also examined the production of methane and CO_2 by resting cell suspensions incubated with various substrates (Tables 2 and 3). The P_{tet} *vht* and P_{tet} *vht* Δ*ech* mutants were not examined because they do not grow in any medium under noninducing conditions. Similarly, we did not assay the production of methane from acetate, because prior growth on acetate is required to induce the enzymes needed for this activity and most of the hydrogenase mutants are unable to grow under these conditions (20, 21).

Consistent with their lack of growth phenotypes, the Δ*fre* and Δ*vhx* single mutations did not affect the levels of methane produced from any substrate tested. These mutations also did not affect the ratio of methane/CO_2 produced from methanol or from methanol-H_2. However, the Δ*vhx* mutation lowered the rate of methane production. The Δ*fre* mutation also lowered the rate of methane production, but only when it was combined with the Δ*frh* mutation.

TABLE 3 Rate of CH_4 production from resting cell suspensions of *M. barkeri* mutant strains

Genotype	Rate of CH_4 production (nmol min^{-1} mg^{-1})	
	Methanol	Methanol and H_2
Δ*hpt*[a]	86 ± 7	132 ± 18
Δ*fre*	84 ± 1	123 ± 16
Δ*vhx*	71 ± 2	74 ± 12
Δ*ech*	57 ± 5	122 ± 7
Δ*ech* Δ*frh*	20 ± 1	27 ± 3
Δ*ech* Δ*frh* Δ*vht*	31 ± 2	30 ± 3
Δ*ech* Δ*frh* Δ*fre* Δ*vht-vhx*[b]	19 ± 2	19 ± 2
Δ*frh*	23 ± 1	136 ± 9
Δ*frh* Δ*fre*	14 ± 1	87 ± 3
Δ*frh* Δ*vht*	38 ± 8	36 ± 4
Δ*frh* Δ*fre* Δ*vht-vhx*[b]	32 ± 10	34 ± 13

[a]The genotype of the *M. barkeri* Fusaro parental strain.
[b]*Mbar_A1842* and *Mbar_1843* were also deleted.

As seen in previous studies, the Δ*ech* mutants produced only minor amounts of methane from H_2-CO_2 (<2% relative to the amount produced by the parental strain) but produced wild-type levels from both methanol and methanol-H_2. During incubations with methanol, methane and CO_2 were produced in a 3:1 ratio, consistent with disproportionation of the substrate via the methylotrophic pathway (Fig. 2). Cell suspensions incubated with methanol and H_2 produced only methane, showing that addition of hydrogen inhibits methanol oxidation. The rate of methane production by the Δ*ech* mutant was somewhat lower than that of the wild type using both methanol and methanol-H_2. This rate was further reduced when the *ech* deletion was combined with mutations removing the *frh* or *vht* operon. Accordingly, the Δ*ech* Δ*frh* double mutant produced methane nearly 5 times slower than the wild-type strain. Interestingly, this mutant produced a small amount of CO_2, in addition to the wild-type level of methane, indicating that a small amount of methanol was oxidized. When the *ech*, *frh*, and *vht* hydrogenases were deleted together, the quantity and stoichiometry of methane and CO_2 production were identical to those observed on methanol alone.

The Δ*frh* single mutant produced levels and ratios of methane and CO_2 similar to those produced by the parental strain with methanol or methanol-H_2. When H_2-CO_2 was the substrate, methane production was reduced ca. 10-fold but, significantly, was not abolished. Combining the Δ*frh* mutation with deletions of *vht* and *ech* reduced methane production from H_2-CO_2 to negligible levels. In contrast, minimal effects on methane and CO_2 production or stoichiometry were observed when methanol was the sole substrate. However, when combined with the deletion of *vht* or *ech*, the Δ*frh* mutants produced significant levels of CO_2 when incubated with methanol-H_2, and the triple Δ*ech* Δ*frh* Δ*vht* mutant produced levels similar to those seen in assays when it was incubated with methanol alone. The rates of methane production were substantially lower than those by the wild type for all Δ*frh* mutants.

Enzyme activity in hydrogenase mutants. The hydrogenase activity for selected deletion mutants was measured in the forward direction (H_2 oxidation) to allow estimation of the contributions of each enzyme to overall activity (Table 4).

The hydrogenase activity of mutants lacking Fre or Vhx was not statistically significantly different from that of the parental strain. Moreover, the hydrogenase activity of the Δ*ech* Δ*frh* Δ*vht* mutant, which still encodes Fre and Vhx, was not statistically significantly different from that of the Δ*ech* Δ*frh* Δ*fre* Δ*vht-vhx* mutant, which lacks all five hydrogenase operons. Thus, the *freAEGB* and *vhxGAC* operons do not, by themselves, produce detectable levels of hydrogenase. Because Fre and Vhx are essentially inactive, the hydrogenase levels in the Δ*frh* Δ*vht* and Δ*ech* Δ*frh* strains can be attributed solely to Ech and Vht, respectively. Accordingly, Ech has the lowest activity of the three hydrogenases, accounting for ca. 4% of total activity, with Vht activity being ca. 6-fold higher. Consistent with this conclusion, deletion of *ech* did not significantly affect

TABLE 4 Hydrogenase activity of *M. barkeri* mutant strains

Genotype	Sp act[a]
Δ*hpt*[b]	11.10 ± 4.29
Δ*fre*	9.18 ± 4.38
Δ*vhx*	8.51 ± 3.93
Δ*ech* Δ*frh* Δ*vht*	**0.01 ± 0.00**[d]
Δ*ech* Δ*frh* Δ*fre* Δ*vht-vhx*[c]	**0.02 ± 0.00**
Δ*ech*	17.13 ± 4.90
Δ*frh* Δ*vht*	**0.42 ± 0.09**
Δ*ech* Δ*frh*	**2.60 ± 1.36**
Δ*frh*	**3.12 ± 1.89**

[a]Specific activity is in micromoles of H_2 oxidized per minute per milligram.
[b]The *M. barkeri* Fusaro parental strain.
[c]*Mbar_A1842* and *Mbar_A1843* were also deleted.
[d]Values that are significantly different ($P < 0.01$) from the value for the Δ*hpt* parental strain are indicated in bold.

hydrogenase activity, whereas the Δ*frh* strain had drastically diminished activity compared to the parental strain. Additionally, the activity from the Δ*frh* strain, which encodes both Vht and Ech, was roughly equivalent to the combined activities of strains encoding only Vht or only Ech. Because strains expressing only Frh hydrogenase are inviable, the activity of this hydrogenase cannot be directly determined from a mutant strain. However, the relative contribution of Frh can be estimated from the hydrogenase activities of other mutants. Thus, by subtracting the activities of Vht and Ech from the activity of the parental strain, we estimate that roughly 75% of the hydrogenase activity can be attributed to Frh.

Effect of hydrogenase deletions on mRNA abundance. Our estimate of the relative activities of the individual hydrogenases assumes that the expression levels for each hydrogenase are unaffected by deletion of the others. To explicitly examine this possibility, we determined the global mRNA abundance profiles for each mutant using RNA sequencing (RNA-seq) (Table S4 and Data Set S1). Importantly, the RNA used in this analysis was isolated from the same cultures that were assayed for hydrogenase activity.

As expected, the mRNA levels for the deleted genes in each mutant were significantly and substantially lower than those in the parental strain, providing an important validation that the correct strains were used in these assays. Moreover, no significant differences in mRNA abundance from that of the parent were observed for the remaining hydrogenases in any strain, showing that the expression of individual hydrogenase operons is not regulated by the presence/absence of other hydrogenase genes. Thus, the hydrogenase activities found in the various mutants accurately reflect the combined activities of each enzyme in all strains.

Large numbers of *M. barkeri* genes showed significant changes in mRNA abundance in the hydrogenase mutants relative to the parental strain. Accordingly, 2.7% of all genes were differently regulated in strains with one or two deleted hydrogenases, whereas the Δ*ech* Δ*frh* Δ*vht* and Δ*ech* Δ*frh* Δ*fre* Δ*vht-vhx* strains showed 17.4% and 22.5% differently regulated genes, respectively (Data Set S1). Of these, most encode proteins with unknown functions or with annotated functions that do not appear to be related to energy conservation. One exception was the gene for the F_{420} dehydrogenase (*fpo*), whose mRNA abundance increased significantly in all strains lacking *frh* (Table S4). This result suggests that the cell has a mechanism to sense the redox state of F_{420}, which is altered upon deletion of *frh*.

DISCUSSION

While fully consistent with the proposed functions of the *M. barkeri* hydrogenases, our phenotypic characterization of mutants lends new insight into the flexibility and interconnected nature of methanogenic metabolism. For example, reduction of CO_2 to CH_4 is expected to require three kinds of electron donors: Fd_{red}, $F_{420/red}$, and reduced methanophenazine (1). Consistent with this idea, mutants lacking hydrogenases that

reduce Fd (Ech), F_{420} (Frh), or methanophenazine (Vht) are unable to grow on H_2-CO_2 (Table 1; see also Fig. S2 in the supplemental material). Thus, we were surprised to observe the production of methane from H_2-CO_2 in cell suspensions of Δ*frh* mutants. Assuming that this process involves the standard CO_2 reduction pathway, this would require an alternative source of $F_{420/red}$ for the reduction of methenyl- and methylene-tetrahydrosarcinapterin (Fig. 2). Two alternative sources can be envisioned: first, Fpo could produce $F_{420/red}$ (standard reduction potential [E_0'] = −360 mV) using reduced methanophenazine (E_0' = −165 mV) as the electron donor via reverse electron transport driven by the proton motive force; second, a soluble heterodisulfide reductase could produce $F_{420/red}$ via electron bifurcation using CoM-S-S-CoB and Fd_{red} as the substrates (as suggested previously [22, 23]). In the former mechanism, reduced methanophenazine would be derived from H_2 using Vht; in the latter, Fd_{red} would be derived from H_2 via Ech. Interestingly, double mutants lacking Frh and either Ech or Vht produce much less methane than the Δ*frh* single mutant; thus, both alternate pathways may contribute to this phenotype. The inability of the Δ*frh* mutant to grow on H_2-CO_2 suggests that this alternate methane-producing pathway does not provide sufficient energy for growth or that it fails to provide an essential biosynthetic precursor.

Similar metabolic flexibility is seen during methylotrophic methanogenesis, which can occur via H_2-dependent or -independent mechanisms (Fig. 2 and 3) (11, 12, 15, 16). We previously showed that a hydrogen cycling mechanism involving Frh and Vht is the preferred mode of electron transport in *M. barkeri*. Nevertheless, *M. barkeri* is also capable of methylotrophic growth in the absence of Frh and Vht (11, 15). Data reported here reveal that methylotrophic growth in *M. barkeri* is possible when all three hydrogenases are deleted (Table 1; Fig. S2). Thus, we have created an *M. barkeri* strain similar to *Methanosarcina acetivorans*, which has no detectable hydrogenase activity but which grows well on methylotrophic substrates (7, 14). During methylotrophic growth in *M. acetivorans*, an electron transport chain comprised of Fpo and HdrDE is used to capture energy from the $F_{420/red}$ produced by the oxidative branch of the methanogenic pathway (Fig. 2 and 3). Our genetic analyses suggest that Fpo is also used to metabolize $F_{420/red}$ in *M. barkeri* Δ*frh* Δ*vht* mutants (11, 15). The oxidative branch of the methylotrophic pathway also produces Fd_{red}, which in *M. acetivorans* is oxidized by a membrane-bound, ion-pumping Fd_{red}:methanophenazine oxidoreductase known as Rnf (24). However, because *M. barkeri* does not encode Rnf, this energy-conserving electron transport pathway is not available to the Ech mutants characterized here. Thus, an alternative Fd_{red}:heterodisulfide oxidoreductase system must exist to allow the growth of these mutants on methanol. It has been suggested that this alternate Fd_{red}:heterodisulfide oxidoreductase activity is catalyzed by a cytoplasmic, electron-bifurcating heterodisulfide reductase (HdrABC) similar to the electron-bifurcating heterodisulfide reductase of non-cytochrome-containing methanogens (Fig. 3) (22). Biochemical data from a homologous *M. acetivorans* enzyme support this possibility (23).

Interestingly, the stoichiometry of the methane and CO_2 produced from methanol-H_2 in the Δ*frh* Δ*vht* and Δ*frh* Δ*fre* Δ*vht-vhx* mutants lends additional support for an alternate Fd_{red}:heterodisulfide oxidoreductase. These strains, which encode only Ech, might be expected to disproportionate methanol to CH_4 and CO_2 in a 3:1 ratio, as was seen in the strains lacking all three active hydrogenases. Instead, they produced CH_4 and CO_2 at an approximate ratio of 10:1, suggesting that a substantial portion of the methanol was reduced directly to CH_4 using electrons obtained by H_2 oxidation. Because Ech is the sole remaining hydrogenase in these strains, electrons from Fd_{red} must be involved in this process.

H_2 also inhibits the oxidation of methanol when both substrates are present via a mechanism that is clearly mediated by hydrogenase activity. Accordingly, in the presence of H_2, methanol is solely reduced to methane by cell suspensions of strains that contain all three hydrogenases, while it is disproportionated to methane and CO_2 in a 3:1 ratio when all three are absent. The hydrogenase-mediated inhibition of methanol oxidation is graded, with Vht having the largest effect and Ech having the

smallest. Similarly, Ech mutants are able to grow on methanol-H_2 only when they are supplemented with biosynthetic precursors, which has been interpreted to mean that they cannot produce the reducing equivalents needed for biosynthesis by oxidizing methanol to CO_2 (16). We showed here that this effect is alleviated by deletion of genes encoding Frh and Vht, with the Δ*vht* mutation having a much larger effect. Because protein synthesis was blocked by addition of puromycin in the cell suspension experiments, these effects could not have been mediated by changes in the concentration of enzymes in the methanogenic pathways. Moreover, because inhibition requires the hydrogenase enzymes to be present, it is likely that a product of the enzymatic reaction, namely, the reduced enzyme cofactors, mediates inhibition. Thus, in the presence of high H_2 partial pressures and the appropriate hydrogenase, we would expect oxidized methanophenazine, oxidized F_{420} ($F_{420/ox}$), and oxidized Fd (Fd_{ox}) to be kept at very low levels. Interestingly, the graded inhibition in response to the loss of Vht, Frh, and Ech mimics the thermodynamics of the hydrogenase reactions, with methanophenazine being the most energetically favorable electron acceptor and Fd being the least. This suggests at least two possible mechanisms to account for the inhibition: (i) allosteric inhibition or covalent inactivation of a key enzymatic step in the oxidative branch of the pathway, which could be triggered by one or more reduced cofactors, or (ii) simple changes in the availability of $F_{420/ox}$ and Fd_{ox}, which are needed for three discrete steps in the oxidative branch of the methyloptrophic pathway (Fig. 2). Note that in the second mechanism, the major inhibitory effect of Vht on methyl oxidation can be explained only if high levels of reduced methanophenazine influence the levels of $F_{420/ox}$, which could occur by changing the equilibrium of the Fpo reaction (Fig. 2 and 3).

In addition to affecting flux through methanogenic pathways, the levels of reduced or oxidized cofactors may be used as a sensory input to modulate gene regulation. Transcriptional profiling of hydrogenase mutants showed that in all strains lacking *frh*, the *fpo* operon was significantly upregulated. Without Frh, Fpo is solely responsible for the $F_{420/red}$: methanophenazine oxidoreductase activity required to transfer electrons from the oxidative to reductive portions of the methylotrophic electron transport pathway. The elevated abundance of *fpo* mRNA in Δ*frh* strains indicates that the cell has a mechanism to sense and respond to an F_{420} redox imbalance. A previous study identified MreA as a global regulator in *Methanosarcina* with the ability to bind and repress the *fpo* promoter region during aceticlastic growth (25). This regulator was shown to affect gene expression based on the growth substrate; however, the mechanism and sensory input are unknown. Systems for gene regulation based on the detected redox imbalance of F_{420} and other electron carriers are a potential source for future studies.

The levels of hydrogenase activity for the three enzyme types have significant ramifications for the hydrogen cycling model on energy conservation (15). We have shown that Δ*vht* mutations are lethal when Frh is present but not when it is absent. Moreover, when *vht* expression is turned off using a regulated promoter, cell lysis is concomitant with H_2 accumulation, implying that the inability to recapture the H_2 produced in the cytoplasm is responsible for the lethal phenotype. With this in mind, it seems clear that the cytoplasmic activities of Frh must be carefully balanced against the periplasmic activity of Vht. Interestingly, our data show that the activity of Frh is ca. 3-fold higher than that of Vht. Thus, it appears that the ability of Frh to produce H_2 is much higher than the ability of Vht to take it up. We recognize that our assays were not conducted with the native substrates (which are not commercially available); therefore, we approximated the *in vivo* activity of each enzyme based on available literature values determined in assays in which a variety of natural and artificial cofactors were used (Table S5). These data suggest that the relative activities of Frh and Vht are more similar than our assay data suggest, with Frh activity being ca. 1.5-fold higher than Vht activity. While this extrapolation must be interpreted with caution, it still suggests that the capacity of Frh is higher than that of Vht. In this regard, both Vht and Ech are coupled to the ion motive force; thus, activity in whole, metabolically active cells could be substantially different.

Finally, unlike Frh and Vht, Fre and Vhx are not able to provide sufficient levels of $F_{420/red}$ and reduced methanophenazine, respectively, for growth via CO_2 reduction. Additionally, the Δ*ech* Δ*frh* Δ*vht* strain, which encoded only the Fre and Vhx hydrogenases, had no detectable hydrogenase activity. This could be due to the low expression of the *fre* and *vhx* operons, the absence of posttranslational processing, mutations in structural or catalytic residues, or some combination of these (7). Analysis of RNA sequencing data from wild-type *M. barkeri* grown methylotrophically indicated that the mRNA abundance of *fre* was approximately 50-fold lower than that of *frh* (Data Set S1), similar to the relative abundance observed by Vaupel and Thauer (8). Additionally, the abundance of *vhx* transcripts was more than 200-fold lower than that of *vht* transcripts. We note that our enzymatic assays would have easily detected hydrogenase activity at levels 200-fold lower than those that we observed for the strains encoding only *vht*. Thus, poor gene expression cannot explain the lack of activity in strains expressing only Fre or Vhx. Hydrogenases require several maturation steps to become active enzymes, including processing by the maturation proteases encoded by the *frhD* and *vhtD* genes. Thus, it remains possible that Fre and Vhx genes encode active enzymes if FrhD and VhtD are *trans*-acting maturation proteases. Given that the mutants characterized here removed the entire *frh* and *vht* operons, our data do not address this possibility.

MATERIALS AND METHODS

Media and growth conditions. *Methanosarcina* strains were grown as single cells (26) at 37°C in high-salt (HS) broth medium (27) or on agar-solidified medium as described previously (28). The growth substrates provided were methanol (125 mM in broth medium and 50 mM in agar-solidified medium) or sodium acetate (120 mM) under a headspace of N_2-CO_2 (80:20, vol/vol) at 50 kPa over ambient pressure, H_2-CO_2 (80:20, vol/vol) at 300 kPa over ambient pressure, or a combination of methanol plus hydrogen. Cultures were supplemented as indicated above with 0.1% yeast extract (YE), 0.1% Casamino Acids (CAA), 10 mM sodium acetate, 10 mM pyruvate, or 100 mM pyruvate. Puromycin (Calbiochem, San Diego, CA) was added at 2 μg ml^{-1} for selection of the puromycin transacetylase (*pac*) gene (29). 8-Aza-2,6-diaminopurine (8-ADP; Sigma, St. Louis, MO) was added at 20 μg ml^{-1} for selection against the presence of *hpt* (29). Tetracycline (Tet) was added at 100 μg ml^{-1} to induce the tetracycline-regulated P*mcrB*[*tet*(O1)] promoter (19). Standard conditions were used for the growth of *Escherichia coli* strains (30) DH5α λ *pir* (31) and DH10B (Stratagene, La Jolla, CA), which were used as the hosts for plasmid constructions.

DNA methods and plasmid constructions. Standard methods were used for plasmid DNA isolation and manipulation in *E. coli* (32). Liposome-mediated transformation was used for *Methanosarcina* as described previously (33). Genomic DNA isolation and DNA hybridization were as described previously (27, 28, 34). DNA sequences were determined from double-stranded templates by the W. M. Keck Center for Comparative and Functional Genomics, University of Illinois. Plasmid constructions are described in Tables S1 and S2 in the supplemental material.

Strain construction in *M. barkeri*. The construction and genotypes of all *Methanosarcina* strains are presented in Table S3. Hydrogenase-encoding genes were deleted sequentially in a specific order (Fig. S1) because certain hydrogenase deletion mutants are viable only when other hydrogenase genes are deleted first (15). To simplify isolation of strains that lack the hydrogenase operons *vhxGAC* and *vhtGACD*, the genes between the two operons (*Mbar_A1842* and *Mbar_A1843*) were also deleted (Fig. 1). All mutants were confirmed by either PCR or DNA hybridization (Fig. S3 to S6).

Determination of growth characteristics. For growth rate determinations, cultures were grown on methanol or methanol plus H_2-CO_2 (Δ*frh* and Δ*frh* Δ*fre* strains) to mid-log phase (optical density at 600 nm [OD_{600}], ca. 0.5). An approximately 3% inoculum of the culture (or 10%, in the case of acetate) was then transferred to fresh medium in at least four replicates and incubated at 37°C. Growth was quantified by measuring the OD_{600}. With the exception of samples grown on acetate, all OD_{600} values were measured with a Spectronic 20 spectrophotometer (Thermo Fisher Scientific, Waltham, MA); the OD_{600} values of samples grown on acetate were measured with a Hewlett Packard 8453 spectrophotometer (Agilent, Santa Clara, CA). Note that an OD of 1.0 on the Hewlett Packard 8453 spectrophotometer is equivalent to an OD of ~0.2 on the Spectronic 20 spectrophotometer. Generation times were calculated during exponential growth phase, and the lag phase was defined as the time required to reach a half-maximal OD_{600}.

Cell suspension experiments. Cells grown on methanol or methanol plus H_2-CO_2 (Δ*frh* and Δ*frh* Δ*fre* strains) were collected in late exponential phase (OD_{600} = 0.6 to 0.7) by centrifugation at 5,000 × *g* for 15 min at 4°C. The cells were washed once with anaerobic HS PIPES [piperazine-*N*,*N*′-bis(2-ethanesulfonic acid)] buffer (50 mM PIPES at pH 6.8, 400 mM NaCl, 13 mM KCl, 54 mM $MgCl_2$, 2 mM $CaCl_2$, 2.8 mM cysteine, 0.4 mM Na_2S) and resuspended in the same buffer to a final concentration of 10^9 cells/ml. Cells were counted visually using a Petroff-Hausser counting chamber (Hausser Scientific, PA). All assay mixtures contained 2 ml of the suspension, and the assays were conducted under strictly anaerobic conditions in 25-ml Balch tubes sealed with butyl rubber stoppers using 250 mM methanol as the methanogenic substrate under a headspace of N_2, H_2, or H_2-CO_2 (80/20%) at 250 kPa over the ambient pressure, as indicated where appropriate. Puromycin (20 μg/ml) was added to prevent protein synthesis.

Cells were held on ice until initiation of the assay by transfer to 37°C. For rate determination, gas phase samples were withdrawn at various time points and assayed for CH_4 by gas chromatography (GC) at 225°C in a Hewlett Packard gas chromatograph (5890 series II) equipped with a flame ionization detector. The column used was stainless steel and was filled with 80/120 Carbopack B–3% SP-1500 (Supelco, Bellefonte, PA), and helium was the carrier gas. For total CH_4 and CO_2 production, the assay mixtures were incubated at 37°C for 36 h prior to withdrawal of gas-phase samples for analysis by GC at 225°C in a Hewlett Packard gas chromatograph (5890 Series II) equipped with a thermal conductivity detector. A stainless steel 60/80 Carboxen-1000 column (Supelco, Bellefonte, PA) with helium as the carrier gas was used. Total cell protein was determined using the Bradford method (35) after 1 ml of the cells was lysed by resuspension in double-distilled H_2O with 1 μg/ml RNase and DNase.

Hydrogenase assays. Strains were grown at 37°C in HS medium supplemented with 125 mM methanol, and cells were harvested from 10 ml mid-exponential-phase culture by centrifugation at 1,228 $\times$ *g* for 15 min in an IEC MediSpin (Needham Heights, MA) benchtop centrifuge. Preparation of the cell extract was performed in an anaerobic chamber under an atmosphere of H_2-N_2 (4%/96%). Cells were washed once in 10 ml HS-MOPS (morpholinepropanesulfonic acid) (2 mM dithiothreitol [DTT], 400 mM NaCl, 13 mM KCl, 54 mM $MgCl_2$, 2 mM $CaCl_2$, 50 mM MOPS, pH 7.0) and lysed in 1 ml lysis buffer (2 mM DTT, 0.5% *n*-dodecyl β-D-maltoside, ca. 50 Kunitz units bovine pancreas DNase I, 50 mM MOPS, pH 7.0) on ice for 30 min. Enzyme-containing supernatant was separated from the cell debris by centrifugation at 13,600 $\times$ *g* for 2.5 min (model 235C microcentrifuge; Fisher Scientific, Waltham, MA). The protein concentration was measured via the Bradford method (35).

Assays were performed anaerobically in 1.7-ml quartz cuvettes sealed with rubber stoppers. A total reaction volume of 1 ml was used and included the cell extract mixed with 50 mM MOPS buffer (pH 7.0) containing 2 mM DTT and 2 mM benzyl viologen (BV). The cuvette headspace was pressurized to 30 kPa with 100% H_2 after being flushed for 2 min. Cuvettes with the reaction mixture were prewarmed to 30°C before the reaction was initiated by the addition of BV. Hydrogenase activity was determined by quantifying the change in the absorbance of BV at 578 nm (extinction coefficient, 8.65 cm^{-1} mM^{-1}) with a Cary 50 UV-visible spectrophotometer (Agilent, Santa Clara, CA). One unit of hydrogenase activity was defined as the oxidation of 1 μmol H_2 per minute, based on the fact that 2 μmol BV is reduced for each μmol H_2 oxidized. A minimum of three independent measurements from biological replicates was performed for each strain.

RNA sequencing. Immediately prior to cell harvest for hydrogenase assays, 2.5 ml of the same culture was harvested for total RNA isolation. An equal volume of the TRIzol reagent (Ambion, Carlsbad, CA) was added to the culture to lyse the cells, and samples were incubated at room temperature for 5 min. RNA was then isolated with a Direct-zol RNA MiniPrep kit from Zymo Research (Irvine, CA) according to the manufacturer's directions. RNA samples were stored at −80°C.

To increase the coverage of mRNA during sequencing, rRNA was removed from samples via subtractive hybridization. The method of Stewart et al. (36) was utilized with the following modifications. Templates for 16S and 23S rRNA probes were generated by PCR from strain WWM85 with primers 16SFor, T716SRev, 23SFor, and T723SRev. *In vitro* transcription with a MEGAscript high-yield transcription kit (Ambion) was used for the production of biotinylated antisense rRNA probes from 400 ng of the purified PCR products in separate reactions. After removal of the template with DNase I, probes were purified with a Zymo Research RNA Clean & Concentrator kit. Hybridization reactions (30 μl) for each sample contained the following: 20% formamide, 1$\times$ SSC buffer (1$\times$ SSC buffer is 0.15 M NaCl plus 0.015 M sodium citrate), 20 U SUPERase inhibitor, 2 μg total RNA, 4 μg 16S rRNA probe, and 4 μg 23S rRNA probe. The reaction mixtures were denatured at 70°C for 10 min, the temperature was ramped down to 25°C (−0.1°C s^{-1}), and the reaction mixtures were incubated at room temperature for 10 min. rRNA hybridized to the biotinylated probe was removed via streptavidin-coated magnetic beads (New England BioLabs, Ipswich, MA). Beads (500 μl per sample) were washed twice with 500 μl 1$\times$ SSC buffer prior to the addition of hybridized RNA sample diluted to 250 μl in 1$\times$ SSC buffer with 20% formamide. Samples were incubated for 1 h at room temperature with gentle shaking before separation of the beads on a magnetic rack. The supernatant was removed, the beads were washed with 250 μl 1$\times$ SSC buffer, and the supernatant and wash were pooled and cleaned with the Zymo Research RNA Clean & Concentrator kit.

Preparation and sequencing of RNA-seq libraries was performed at the Roy J. Carver Biotechnology Center at the University of Illinois at Urbana-Champaign. Libraries were made with a TruSeq Stranded mRNA sample preparation kit, sequenced with a HiSeq 2000 sequencer using a TruSeq SBS (v3) kit, and processed with Casava (v1.8.2) software, all in accordance with the manufacturer's directions (Illumina, San Diego, CA). All sequencing data were further processed and analyzed as previously described (37) with the CLC Genomics Workbench (v7) program (Qiagen). Within this program, the empirical analysis of differential gene expression (EDGE) tool was used for statistical analysis (38). The expression of differently regulated genes was considered significant when they were up- or downregulated at least 3-fold with a *P* value of $\leq$0.05. Three biological replicates were sequenced and analyzed for each strain.

Accession number(s). Raw and processed data have been deposited in the Gene Expression Omnibus (GEO) database under accession number GSE98441.

SUPPLEMENTAL MATERIAL

Supplemental material for this article may be found at https://doi.org/10.1128/JB.00342-18.

SUPPLEMENTAL FILE 1, PDF file, 5.9 MB.

SUPPLEMENTAL FILE 2, XLSX file, 14.1 MB.

ACKNOWLEDGMENT

We acknowledge the Division of Chemical Sciences, Geosciences, and Biosciences, Office of Basic Energy Sciences, of the U.S. Department of Energy for funding this work through grant DE-FG02-02ER15296.

REFERENCES

1. Thauer RK, Hedderich R, Fischer R. 1993. Reactions and enzymes involved in methanogenesis from CO_2 and H_2, p 209–252. *In* Ferry JG (ed), Methanogenesis: ecology, physiology, biochemistry & genetics. Chapman & Hall, New York, NY.
2. Vignais PM, Billoud B, Meyer J. 2001. Classification and phylogeny of hydrogenases. FEMS Microbiol Rev 25:455–501.
3. Peters JW, Schut GJ, Boyd ES, Mulder DW, Shepard EM, Broderick JB, King PW, Adams MWW. 2015. [FeFe]- and [NiFe]-hydrogenase diversity, mechanism, and maturation. Biochim Biophys Acta 1853:1350–1369. https://doi.org/10.1016/j.bbamcr.2014.11.021.
4. Thauer RK, Kaster A-K, Goenrich M, Schick M, Hiromoto T, Shima S. 2010. Hydrogenases from methanogenic archaea, nickel, a novel cofactor, and H_2 storage. Annu Rev Biochem 79:507–536. https://doi.org/10.1146/annurev.biochem.030508.152103.
5. Thauer RK, Kaster A-K, Seedorf H, Buckel W, Hedderich R. 2008. Methanogenic archaea: ecologically relevant differences in energy conservation. Nat Rev Microbiol 6:579–591. https://doi.org/10.1038/nrmicro1931.
6. Lie TJ, Costa KC, Lupa B, Korpole S, Whitman WB, Leigh JA. 2012. Essential anaplerotic role for the energy-converting hydrogenase Eha in hydrogenotrophic methanogenesis. Proc Natl Acad Sci U S A 109:15473–15478. https://doi.org/10.1073/pnas.1208779109.
7. Guss AM, Kulkarni G, Metcalf WW. 2009. Differences in hydrogenase gene expression between *Methanosarcina acetivorans* and *Methanosarcina barkeri*. J Bacteriol 191:2826–2833. https://doi.org/10.1128/JB.00563-08.
8. Vaupel M, Thauer RK. 1998. Two F_{420}-reducing hydrogenases in *Methanosarcina barkeri*. Arch Microbiol 169:201–205. https://doi.org/10.1007/s002030050561.
9. Fiebig K, Friedrich B. 1989. Purification of the F_{420}-reducing hydrogenase from *Methanosarcina barkeri* (strain Fusaro). Eur J Biochem 184:79–88. https://doi.org/10.1111/j.1432-1033.1989.tb14992.x.
10. Michel R, Massanz C, Kostka S, Richter M, Fiebig K. 1995. Biochemical characterization of the 8-hydroxy-5-deazaflavin-reactive hydrogenase from *Methanosarcina barkeri* Fusaro. Eur J Biochem 233:727–735. https://doi.org/10.1111/j.1432-1033.1995.727_3.x.
11. Kulkarni G, Kridelbaugh DM, Guss AM, Metcalf WW. 2009. Hydrogen is a preferred intermediate in the energy-conserving electron transport chain of *Methanosarcina barkeri*. Proc Natl Acad Sci U S A 106:15915–15920. https://doi.org/10.1073/pnas.0905914106.
12. Meuer J, Bartoschek S, Koch J, Künkel A, Hedderich R. 1999. Purification and catalytic properties of Ech hydrogenase from *Methanosarcina barkeri*. Eur J Biochem 265:325–335. https://doi.org/10.1046/j.1432-1327.1999.00738.x.
13. Liu Y, Whitman WB. 2008. Metabolic, phylogenetic, and ecological diversity of the methanogenic Archaea. Ann N Y Acad Sci 1125:171–189. https://doi.org/10.1196/annals.1419.019.
14. Guss AM, Mukhopadhyay B, Zhang JK, Metcalf WW. 2005. Genetic analysis of *mch* mutants in two *Methanosarcina* species demonstrates multiple roles for the methanopterin-dependent C-1 oxidation/reduction pathway and differences in H_2 metabolism between closely related species. Mol Microbiol 55:1671–1680. https://doi.org/10.1111/j.1365-2958.2005.04514.x.
15. Kulkarni G, Mand TD, Metcalf WW. 2018. Energy conservation via hydrogen cycling in the methanogenic archaeon *Methanosarcina barkeri*. mBio 9:e01256-18. https://doi.org/10.1128/mBio.01256-18.
16. Meuer J, Kuettner HC, Zhang JK, Hedderich R, Metcalf WW. 2002. Genetic analysis of the archaeon *Methanosarcina barkeri* Fusaro reveals a central role for Ech hydrogenase and ferredoxin in methanogenesis and carbon fixation. Proc Natl Acad Sci U S A 99:5632–5637. https://doi.org/10.1073/pnas.072615499.
17. Deppenmeier U. 2004. The membrane-bound electron transport system of *Methanosarcina* species. J Bioenerg Biomembr 36:55–64. https://doi.org/10.1023/B:JOBB.0000019598.64642.97.
18. Welte C, Deppenmeier U. 2014. Bioenergetics and anaerobic respiratory chains of aceticlastic methanogens. Biochim Biophys Acta 1837:1130–1147. https://doi.org/10.1016/j.bbabio.2013.12.002.
19. Guss AM, Rother M, Zhang JK, Kulkarni G, Metcalf WW. 2008. New methods for tightly regulated gene expression and highly efficient chromosomal integration of cloned genes for *Methanosarcina* species. Archaea 2:193–203. https://doi.org/10.1155/2008/534081.
20. Krzycki JA, Wolkin RH, Zeikus JG. 1982. Comparison of unitrophic and mixotrophic substrate metabolism by acetate-adapted strain of *Methanosarcina barkeri*. J Bacteriol 149:247–254.
21. Jablonski PE, DiMarco AA, Bobik TA, Cabell MC, Ferry JG. 1990. Protein content and enzyme activities in methanol- and acetate-grown *Methanosarcina thermophila*. J Bacteriol 172:1271–1275. https://doi.org/10.1128/jb.172.3.1271-1275.1990.
22. Buan NR, Metcalf WW. 2010. Methanogenesis by *Methanosarcina acetivorans* involves two structurally and functionally distinct classes of heterodisulfide reductase. Mol Microbiol 75:843–853. https://doi.org/10.1111/j.1365-2958.2009.06990.x.
23. Yan Z, Wang M, Ferry JG. 2017. A ferredoxin- and $F_{420}H_2$-dependent, electron-bifurcating, heterodisulfide reductase with homologs in the domains Bacteria and Archaea. mBio 8:e02285-16. https://doi.org/10.1128/mBio.02285-16.
24. Li Q, Li L, Rejtar T, Lessner DJ, Karger BL, Ferry JG. 2006. Electron transport in the pathway of acetate conversion to methane in the marine archaeon *Methanosarcina acetivorans*. J Bacteriol 188:702–710. https://doi.org/10.1128/JB.188.2.702-710.2006.
25. Reichlen MJ, Vepachedu VR, Murakami KS, Ferry JG. 2012. MreA functions in the global regulation of methanogenic pathways in *Methanosarcina acetivorans*. mBio 3:e00189-12. https://doi.org/10.1128/mBio.00189-12.
26. Sowers KR, Boone JE, Gunsalus RP. 1993. Disaggregation of *Methanosarcina* spp. and growth as single cells at elevated osmolarity. Appl Environ Microbiol 59:3832–3839.
27. Metcalf WW, Zhang JK, Shi X, Wolfe RS. 1996. Molecular, genetic, and biochemical characterization of the *serC* gene of *Methanosarcina barkeri* Fusaro. J Bacteriol 178:5797–5802. https://doi.org/10.1128/jb.178.19.5797-5802.1996.
28. Boccazzi P, Zhang JK, Metcalf WW. 2000. Generation of dominant selectable markers for resistance to pseudomonic acid by cloning and mutagenesis of the *ileS* gene from the archaeon *Methanosarcina barkeri* Fusaro. J Bacteriol 182:2611–2618. https://doi.org/10.1128/JB.182.9.2611-2618.2000.
29. Pritchett MA, Zhang JK, Metcalf WW. 2004. Development of a markerless genetic exchange method for *Methanosarcina acetivorans* C2A and its use in construction of new genetic tools for methanogenic archaea. Appl Environ Microbiol 70:1425–1433. https://doi.org/10.1128/AEM.70.3.1425-1433.2004.
30. Wanner BL. 1986. Novel regulatory mutants of the phosphate regulon in *Escherichia coli* K-12. J Mol Biol 191:39–58. https://doi.org/10.1016/0022-2836(86)90421-3.
31. Miller VL, Mekalanos JJ. 1988. A novel suicide vector and its use in construction of insertion mutations: osmoregulation of outer membrane proteins and virulence determinants in *Vibrio cholerae* requires *toxR*. J Bacteriol 170:2575–2583. https://doi.org/10.1128/jb.170.6.2575-2583.1988.
32. Ausubel FM, Brent R, Kingston RE, Moore DD, Seidman JG, Smith JA, Struhl K. 1992. Current protocols in molecular biology. John Wiley & Sons, Inc, New York, NY.
33. Metcalf WW, Zhang JK, Apolinario E, Sowers KR, Wolfe RS. 1997. A genetic system for Archaea of the genus *Methanosarcina*: liposome-mediated transformation and construction of shuttle vectors. Proc Natl Acad Sci U S A 94:2626–2631.
34. Zhang JK, White AK, Kuettner HC, Boccazzi P, Metcalf WW. 2002. Directed mutagenesis and plasmid-based complementation in the methanogenic archaeon *Methanosarcina acetivorans* C2A demonstrated by genetic analysis of proline biosynthesis. J Bacteriol 184:1449–1454. https://doi.org/10.1128/JB.184.5.1449-1454.2002.
35. Bradford MM. 1976. A rapid and sensitive method for the quantita-

tion of microgram quantities of protein utilizing the principle of protein-dye binding. Anal Biochem 72:248–254. https://doi.org/10.1016/0003-2697(76)90527-3.
36. Stewart FJ, Ottesen EA, DeLong EF. 2010. Development and quantitative analyses of a universal rRNA-subtraction protocol for microbial metatranscriptomics. ISME J 4:896–907. https://doi.org/10.1038/ismej.2010.18.
37. Fu H, Metcalf WW. 2015. Genetic basis for metabolism of methylated sulfur compounds in *Methanosarcina* species. J Bacteriol 197:1515–1524. https://doi.org/10.1128/JB.02605-14.
38. Robinson MD, Smyth GK. 2008. Small-sample estimation of negative binomial dispersion, with applications to SAGE data. Biostatistics 9:321–332. https://doi.org/10.1093/biostatistics/kxm030.